Brief Communication

Efficient simultaneous mutagenesis of multiple genes in specific plant tissues by multiplex CRISPR

Norbert Bollier[1,2] (iD), Rafael Andrade Buono[1,2] (iD), Thomas B. Jacobs[1,2,*] (iD) and Moritz K. Nowack[1,2,*] (iD)

[1]Department of Plant Biotechnology and Bioinformatics, Ghent University, Ghent, Belgium
[2]VIB Center for Plant Systems Biology, Ghent, Belgium

CRISPR technology is an established tool for the generation of knockout plants (Zhang *et al.*, 2019), yet limitations remain. First, the manipulation of individual genes may fail to produce phenotypes for groups of genes with redundant or synergistic functions. While this has been partially addressed by multiplexing guide RNAs (gRNAs), there is concern that as the number of targets increases, the chances of obtaining higher-order knock-outs diminish (Zhang *et al.*, 2016). Second, knocking out fundamentally important genes can cause severe pleiotropic phenotypes or lethality. Tissue-specific knockout of genes in somatic tissues can overcome this limitation (Decaestecker *et al.*, 2019; Liang *et al.*, 2019; Wang *et al.*, 2020). However, the efficiency of simultaneously targeting more than three genes in a tissue-specific context is unexplored. Here, by multiplexing gRNAs in *Arabidopsis thaliana* plants expressing Cas9 either ubiquitously (*pPcUBI*) or root cap specifically (*pSMB*), we show that six genes can be simultaneously mutated with high efficiency, generating higher-order mutant phenotypes already in the first transgenic generation (T1). The mutation frequencies for all target genes were positively correlated and unaffected by the order of the gRNAs in the vector, showing that efficient higher-order mutagenesis in specific plant tissues can be readily achieved.

We selected six efficient gRNAs (Decaestecker *et al.*, 2019 and unpublished results) to target the coding sequences of six genes (*GFP*, and the Arabidopsis genes *SMB*, *EXI1*, *GL1*, *ARF7* and *ARF19*; Figure 1a) whose knockout lead to easy-to-score phenotypes in T1 seedlings (*gfp*: loss of GFP signal, *smb*: accumulation of root cap cells (Fendrych *et al.*, 2014), *gl1*: absence of trichomes (Herman and Marks, 1989)) and do not severely affect plant growth or reproduction. Since position effects within gRNA arrays had been a concern regarding mutation efficiency (Zhang *et al.*, 2016), we generated two vectors (hereafter, *pPcUBI(I)* and *pPcUBI (II)*) combining Cas9-mTagBFP2 driven by the ubiquitous *pPcUBI* promoter and the six gRNAs in an inverted order (Figure 1b) and transformed these into an Arabidopsis line with ubiquitous expression of a nuclear-localized GFP (*pHTR5:NLS-GFP-GUS* (Decaestecker *et al.*, 2019) hereafter, NLS-GFP).

Forty-nine out of 96 *pPcUBI(I)* and 52 out of 95 *pPcUBI(II)* T1 seedlings displayed both *gfp* and *smb* phenotypes in roots, indicating simultaneous mutations (Figure 1c,d). Additionally, 44 out of 96 *pPcUBI(I)* and 45 out of 95 *pPcUBI(II)* T1 seedlings also lacked trichomes on the first two true leaves, revealing a high mutation frequency for *GL1*. Altogether, 79% of the *pPcUBI(I)* and 68% of the *pPcUBI(II)* T1 seedlings with at least one detectable knockout phenotype also showed triple *gfp smb gl1* mutant phenotypes. When selecting plants based on the loss of GFP, 90% of the *pPcUBI(I)* and 85% of the *pPcUBI(II)* T1 seedlings displayed triple mutant phenotypes, indicating a strong correlation of mutagenesis efficiencies.

We quantified indel frequencies in 48 *pPcUBI(I)*, 47 *pPcUBI(II)* and a control NLS-GFP plant. The targeted loci were PCR-amplified from root tips and sequenced using Illumina sequencing. Plants showing total or partial *gfp* and *smb* phenotypes had high indel frequencies in *GFP* (27%–100%) and *SMB* (38%–98%), as well as in all other target genes. Hierarchical clustering showed that transgenic T1 plants fell in two major classes that had either high or low levels of mutagenesis for all target genes (Figure 1e). In agreement with previous reports (Feng *et al.*, 2014), 1-bp indels were the predominant repair outcome (50%–80% and 1%–15% respectively), in-frame indels were rare (2%–8%), and 6%–26% of mutations were bigger deletions (>6-bp), insertions (>3-bp) or complex repair outcomes (Figure 1f).

We compared indel frequencies for each target between the two constructs to test the effect of the gRNA position (Figure 1g). The overall indel frequencies were higher for *pPcUBI(II)*, though the difference was only significant for *GFP*. As all other gRNAs had no substantial changes in indel frequencies, our data do not support a position effect in gRNA arrays, thus reducing the complexity of future experimental design.

We then tested whether six genes can be efficiently mutated in a tissue-specific context by making two vectors expressing Cas9-P2A-mTagBFP2 under the root cap-specific *pSMB* promoter with the same arrangement of gRNAs (hereafter, *pSMB(I)* and *pSMB (II)*). Plants were grown in the presence of 1 μM brassinazole (BRZ) to facilitate *smb* phenotyping. This treatment leads to a root covered by living root cap cells in *smb* mutants (Fendrych *et al.*, 2014) and was easily recognizable due to the presence of nuclear mTagBFP2 signal in living root cap cells (Figure 1h).

Thirty-two out of 86 *pSMB(I)* and 46 out of 88 *pSMB(II)* T1 seedlings showed both *gfp* and *smb* phenotypes, as well as a strong mTagBFP2 signal specifically in root cap nuclei as determined by confocal microscopy (Figure 1i). In agreement with our previous report (Decaestecker *et al.*, 2019), mTagBFP2 signal intensity could be used as a proxy for the penetrance of *gfp* and
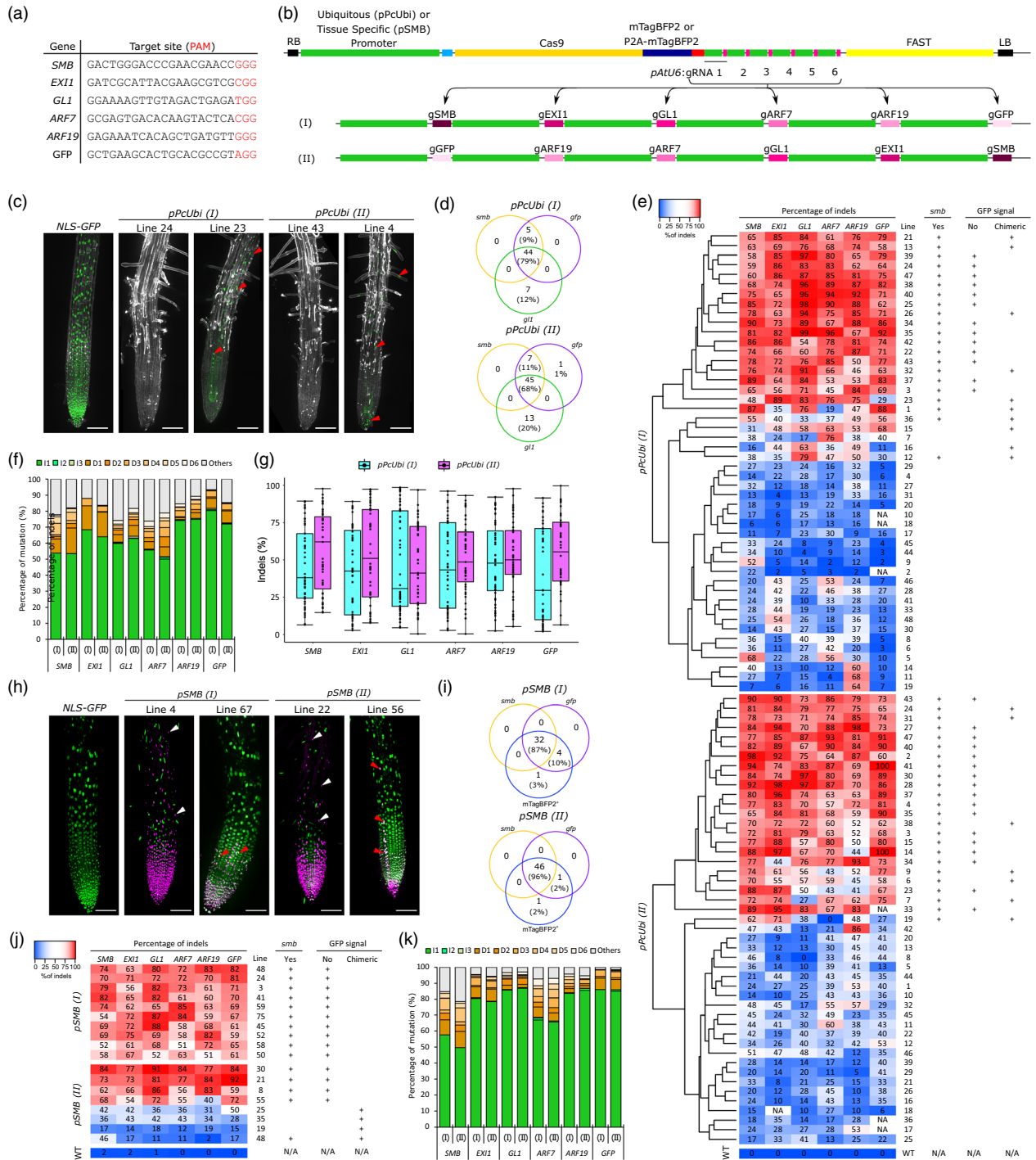
Figure 1 Ubiquitous and root cap-specific knockout of 6 genes in T1 via CRISPR and CRISPR-TSKO. (a) gRNA Target sequences. (b) Diagram of the *pPcUBI* (*Petroselinum crispum* UBIQUITIN promoter) and *pSMB* vectors with gRNAs cloned in an inverted order, *(I)* and *(II)*. (c) Maximum intensity projections of root tips of a representative NLS-GFP seedling, two *pPcUBI(I)* and two *pPcUBI(II)* T1 seedlings showing the complete (left) and chimeric (right) absence of GFP signal and *smb* phenotype. GFP is in green, propidium iodide (PI) in grey. Red arrowheads indicate root cells still expressing GFP. Scale bars, 100 μm. (d) Venn diagram showing the number of plants displaying *smb*, *gfp* and *gl1* mutant phenotype in 96 *pPcUBI(I)* and 95 *pPcUBI(II)* T1 seedlings. (e) Genotype analysis by amplicon sequencing. Phenotypes are indicated on the right panel. (f) Frequency of the main mutation types in both *pPcUBI(I)* and *pPcUBI(II)* plants. I1–I3: 1- to 3-bp insertion, D1–D6: 1- to 6-bp deletion, Others: bigger deletions (>6-bp), insertions (>3-bp) or complex repair outcomes containing both insertions and deletions. (g) Percentage of indels observed in *pPcUBI(I)* and *pPcUBI(II)* T1 plants. (h) Maximum intensity projections of root tips of a representative NLS-GFP seedling, two *pSMB(I)* and two *pSMB(II)* T1 seedlings grown on 1 μM brassinazole showing the complete (left) and chimeric (right) absence of GFP and presence of mTagBFP2 signal specific to root cap cells. GFP is in green, mTagBFP2 in magenta. White arrowheads indicate live root cap cells with nuclear mTagBFP2 signal covering the elongation zone. Red arrowheads indicate root cells still expressing GFP. Scale bars, 100 μm. (i) Venn diagrams showing the number of plants displaying strong mTagBFP2 signal, *smb* and *gfp* phenotype in 86 *pSMB(I)* and 88 *pSMB(II)* T1 seedlings. (j) Genotype analysis of BFP⁺ sorted cells of *pSMB(I)* and *pSMB(II)* T2 seedlings by amplicon sequencing. (k) Frequency of the main mutations types in *pSMB(I)* and *pSMB(II)* plants.

smb knockout phenotypes. To determine mutagenesis efficiency in all target genes specifically in Cas9-expressing root cap cells, we collected root-tip protoplasts expressing mTagBFP2 (BFP$^+$, Cas9 expressing cells) using fluorescence-activated cell sorting from T2 seedlings of ten *pSMB(I)* and eight *pSMB(II)* independent lines. We chose four *pSMB(II)* lines (19, 25, 35 and 48) with weak or chimeric *gfp* and *smb* T1 mutant phenotypes and four *pSMB(I)* and *(II)* lines with highly penetrant *smb* and *gfp* T1 mutant phenotypes.

The targeted loci were PCR-amplified directly from sorted protoplast populations and sequenced by NGS. In *pSMB(I)* and *(II)*, T2 seedlings coming from a T1 parent with strong *smb* and *gfp* phenotypes, the Cas9-expressing BFP$^+$ populations had indel frequencies between 51% and 92% for all six target loci (Figure 1j). As expected, the BFP$^+$ populations of the *pSMB(II)* lines that with weak or chimeric *gfp* and *smb* phenotypes in T1 had lower indel frequencies (2%–50%). These results confirmed that in lines with high *GFP* and *SMB* mutagenesis activity, all genes were simultaneously mutated with high efficiency. Similarly to the ubiquitous lines, the alleles generated were largely consistent across events, with 1-bp indels being the predominant repair outcome (50%–87% and 2%–10%), in-frame insertion or deletions were rare (0%–5%), and 3%–21% of mutations were bigger indels (>3- and >6-bp) or combination of indels (Figure 1k).

In conclusion, we show that ubiquitous CRISPR and CRISPR-TSKO approaches allow fast and simultaneous disruption of six genes in the first transgenic generation with high efficiency. As mutation efficiencies over all loci are correlated, we suggest the use of a target gene with an easy-to-score, non-detrimental loss-of-function phenotype as a proxy for highly mutagenized lines. As an alternative to endogenous genes (Li *et al.*, 2020), loss of GFP in a reporter line can also be used as a proxy. We foresee this approach to be a powerful tool to dissect genetic networks in model and crops species alike.

Acknowledgements

Conflicts of interest

The authors declare no conflict of interest.

Author contributions

N.B., R.A.B., M.K.N. and T.B.J. designed the experiments and wrote the manuscript. N.B. and R.A.B. performed the experiments and analysed the data.

References

Decaestecker, W., Buono, R.A., Pfeiffer, M.L., Vangheluwe, N., Jourquin, J., Karimi, M., Van Isterdael, G. *et al.* (2019) CRISPR-TSKO: a technique for efficient mutagenesis in specific cell types, tissues, or organs in Arabidopsis. *Plant Cell*, **31**, 2868–2887.

Fendrych, M., Van Hautegem, T., Van Durme, M., Olvera-Carrillo, Y., Huysmans, M., Karimi, M., Lippens, S. *et al.* (2014) Programmed cell death controlled by ANAC033/SOMBRERO determines root cap organ size in Arabidopsis. *Curr. Biol.* **24**, 931–940.

Feng, Z., Mao, Y., Xu, N., Zhang, B., Wei, P., Yang, D.L., Wang, Z. *et al.* (2014) Multigeneration analysis reveals the inheritance, specificity, and patterns of CRISPR/Cas-induced gene modifications in Arabidopsis. *Proc. Natl Acad. Sci.* **111**, 4632–4637.

Herman, P.L. and Marks, M.D. (1989) Trichome development in *Arabidopsis thaliana*. II. Isolation and complementation of the GLABROUS1 gene. *Plant Cell*, **1**, 1051–1055.

Li, R., Vavrik, C. and Danna, C.H. (2020) Proxies of CRISPR/Cas9 activity to aid in the identification of mutagenized Arabidopsis plants. *G3 (Bethesda)*, **10**, 2033–2042.

Liang, Y., Eudes, A., Yogiswara, S., Jing, B., Benites, V.T., Yamanaka, R., Cheng-Yue, C. *et al.* (2019) A screening method to identify efficient sgRNAs in Arabidopsis, used in conjunction with cell-specific lignin reduction. *Biotechnol. Biofuels*, **12**, 1–15.

Wang, X., Ye, L., Lyu, M., Ursache, R., Löytynoja, A. and Mähönen, A.P. (2020) An inducible genome editing system for plants. *Nat. Plants*, **6**, 766–772.

Zhang, Y., Malzahn, A.A., Sretenovic, S. and Qi, Y. (2019) The emerging and uncultivated potential of CRISPR technology in plant science. *Nat. Plants*, **5**, 778–794.

Zhang, Z., Mao, Y., Ha, S., Liu, W., Botella, J.R. and Zhu, J.K. (2016) A multiplex CRISPR/Cas9 platform for fast and efficient editing of multiple genes in Arabidopsis. *Plant Cell Rep.* **35**, 1519–1533.